터널과 지하공간, 한국암반공학회지
제13권 제4호, 2003년 8월, pp. 304~315

TUNNEL & UNDERGROUND SPACE, Vol. 13, No. 4, 2003, pp. 304-315
Journal of Korean Society for Rock Mechanics

Modeling the Effect of Geology on Uplift in Concrete Gravity Dam Foundations with the Discontinuous Deformation Analysis

Yong Il Kim[1)]*

불연속 변형 해석을 통한 콘크리트 중력댐 기초에 작용하는 부양력에 대한 지질구조의 영향 모델링

김 용 일

Abstract In this paper, the DDA method with a new hydro-mechanical algorithm is used to study the effect of rock discontinuities on uplift and seepage in concrete gravity dam foundations. This paper presents an alternative method of predicting uplift and seepage at the base of concrete gravity dams. A sensitivity analysis was carried out to study the importance of several parameters on dam stability such as the orientation, spacing, and location of discontinuities. The study shows that joint water flow and adverse geological conditions could result in unusual uplift at the base of concrete gravity dams, well in excess of what is predicted with the classical linear or bi-linear pressure assumption. It is shown that, in general, the DDA program with the hydro-mechanical algorithm can be used as a practical tool in the design of gravity dams built on fractured rock masses.

KeyWords: Discontinuous deformation analysis, Uplift, Fracture, Hydro-mechanical algorithm

초 록 본 논문에서는 수리역학적 알고리즘을 활용한 DDA법을 이용하여 콘크리트 중력댐 기초에서 부양력과 침투에 의한 암반 불연속면의 영향에 대해 연구하였다. 본 논문은 콘크리트 중력댐의 기초에서 부양력과 침투를 예측하는 방법을 보여준다. 댐의 안정성에 미치는 불연속면의 방향, 간격, 위치 등에 대한 변수의 중요성을 연구하기 위하여 민감도 분석이 수행되었다. 본 연구결과 절리를 통한 지하수의 흐름과 좋지 않은 지질학적 조건은 콘크리트 중력댐의 기초에서 전형적인 선형 또는 이중선형 압력 분포의 가정에서 예측한 값을 넘어서는 특별한 부양력의 결과를 나타냈다. 일반적으로, 수리역학적 알고리즘을 활용하는 DDA 프로그램은 균열 암반에 건설되는 중력댐의 설계에 훌륭한 방법으로 이용될 수 있다.

핵심어: 불연속 변형 해석법, 부양력, 균열, 수리역학적 알고리즘

1. Introduction

The Discontinuous Deformation Analysis (DDA) method is a recently developed technique that can be classified as a discrete element method. Shi (1988) first proposed the DDA method in his doctoral thesis; computer programs based on the method were developed and some applications were presented in the thesis as well as in more recent papers. Various modifications to the original DDA formulation have been published in the rock mechanics literature over the past ten years. For instance, Lin (1995) improved the original DDA program of Shi (1988) by including four major extensions: improvement of block interface, calculation of stress distributions within blocks using sub-blocks, block fracturing, and viscoelastic behavior. Although various extensions of the DDA method have been proposed in the literature, its application in rock engineering is still limited. For instance, until recently the method could not be used to model water-block interaction which

[1)]Member, Daewoo E&C Co., LTD.
*교신저자(Corresponding Author): 8915364@mail.dwconst.co.kr
접수일: 2003년 6월 5일
심사 완료일: 2003년 7월 22일

is of particular concern when analyzing the interaction of engineering structures such as dams and tunnels with fractured rock masses. Recently, the authors have been able to incorporate a fully coupled hydro-mechanical algorithm in the DDA method. With that algorithm, the authors were able to analyze the effect of water on tunnel stability (Jang. 2001, Kim et al. 1998, Rouainia et al. 2001).

Current practice in the design of gravity dams is to assume that the uplift pressure at the base of a dam without drains varies linearly from full reservoir pressure at its heel to tailwater pressure at its toe. In the presence of drains, the pressure variation is assumed to be bi-linear. These approximations are based on the assumption that the rock mass behaves like a porous continuum with respect to seepage irrespective of the foundation geology; an assumption that is not always valid if the rock mass contains discrete fractures or geological features. Since the distribution of pressure in a jointed rock mass is controlled almost solely by the properties of the joints, the orientation, spacing and location of discontinuities must influence the uplift pressure in concrete gravity dam foundations.

Several authors have addressed the role of geology on uplift and concrete dam design (Grenoble 1989). In particular, Terzaghi (1929) was the first to explicitly investigate that topic. In one of his many examples, he considered a dam founded on horizontally bedded limestone intersected by a set of widely spaced vertical joints. Terzaghi demonstrated that uplift forces could be influenced by variations in the location of a vertical joint on the downstream side of the dam. He showed, for instance, that uplift force could greatly increase when the vertical joint was located further downstream from the dam. Terzaghi concluded that the most unfavorable conditions were to be found in horizontally stratified geologic deposits with few vertical joints because of the possibility that high uplift pressures could exist over large areas.

Casagrande (1961) presented several idealized cases of how excessive and unfavorable uplift pressures could be created due to unfavorable geological conditions. Three cases were considered: (a) a pervious layer below a dam not fully penetrated by drains, (b) a more pervious layer terminating at the base of a dam, and (c) a horizontal pervious layer not free to drain downstream as it intersects an impervious fault. Stuart (1963) interpreted anomalous uplift pressure measurements at the base of several Corps of Engineers dams based on what was known of their foundation geology. He concluded that high uplift pressures could be found in more massive rocks where the joints were poorly connected.

Serafim and del Campo (1965) derived an analytical solution for the pressure distribution in a tapered crack with an aperture decreasing in the direction of flow. They indicated that the head distribution along a crack of decreasing aperture is always higher than that along a crack of constant aperture. They noted that the condition of decreasing aperture could readily occur in a dam foundation and in particular along the rock-concrete interface.

Grenoble (1989) developed an uncoupled finite element model, and conducted a sensitivity study to determine how uplift at the base of a concrete gravity dam could vary with changes in foundation geology (joint orientation, position of a fault and length of a crack at the base of the dam). Grenoble also investigated how drains and their properties (position, length, diameter, and inclination) could reduce uplift.

Illangasekare et al. (1991) developed a numerical finite element model and conducted parametric studies on the problem of uplift in cracks and the effectiveness of drains in releasing uplift. They noted that drain location has an effect on the pressure distribution and that two opposing phenomena have to be considered in selecting the optimal drain location. On one hand, when a drain is too close to the reservoir, high gradients may cause turbulent flow and increase uplift due to drain choking. On the other hand, for drains located further downstream from the reservoir, drain effectiveness is reduced because the highest reduction in uplift occurs in a zone downstream of the drains.

In this paper, the DDA method with the hydro-mechanical algorithm is used to study the effect of rock discontinuities on uplift and seepage in concrete gravity dam foundations. This paper presents an alternative method of predicting uplift and seepage at

the base of concrete gravity dams using the DDA method.

2. Modeling Water-Block Interaction

A numerical model was developed to study fluid flow in deformable naturally fractured rock masses. The model considers a two-dimensional intact rock mass dissected by a large number of fractures (joints) with variable aperture, length, and orientation. Fluid flow, which occurs when pressure gradients exist, is assumed to be steady, and laminar or turbulent depending on the values of the Reynolds number and the relative roughness of the fracture walls (Louis, 1969). Fluid flow and the rock deformation are fully coupled. Variations in fluid pressure and quantity of fluid result in joint deformation. In turn, joint deformation changes the joint properties, which therefore changes the fluid pressures and the resistance to fluid flow.

2.1 Assumptions

The following assumptions were made when implementing the hydro-mechanical coupling in the DDA program: (a) the fluid is incompressible, (b) the intact rock is impervious, and fluid flow takes place in the joint space only; (c) the rock mass contains a finite number of joints; (d) the intact rock is linearly elastic; and (e) joint displacements are small relative to the joint dimensions.

In the flow model, the fracture space is idealized as

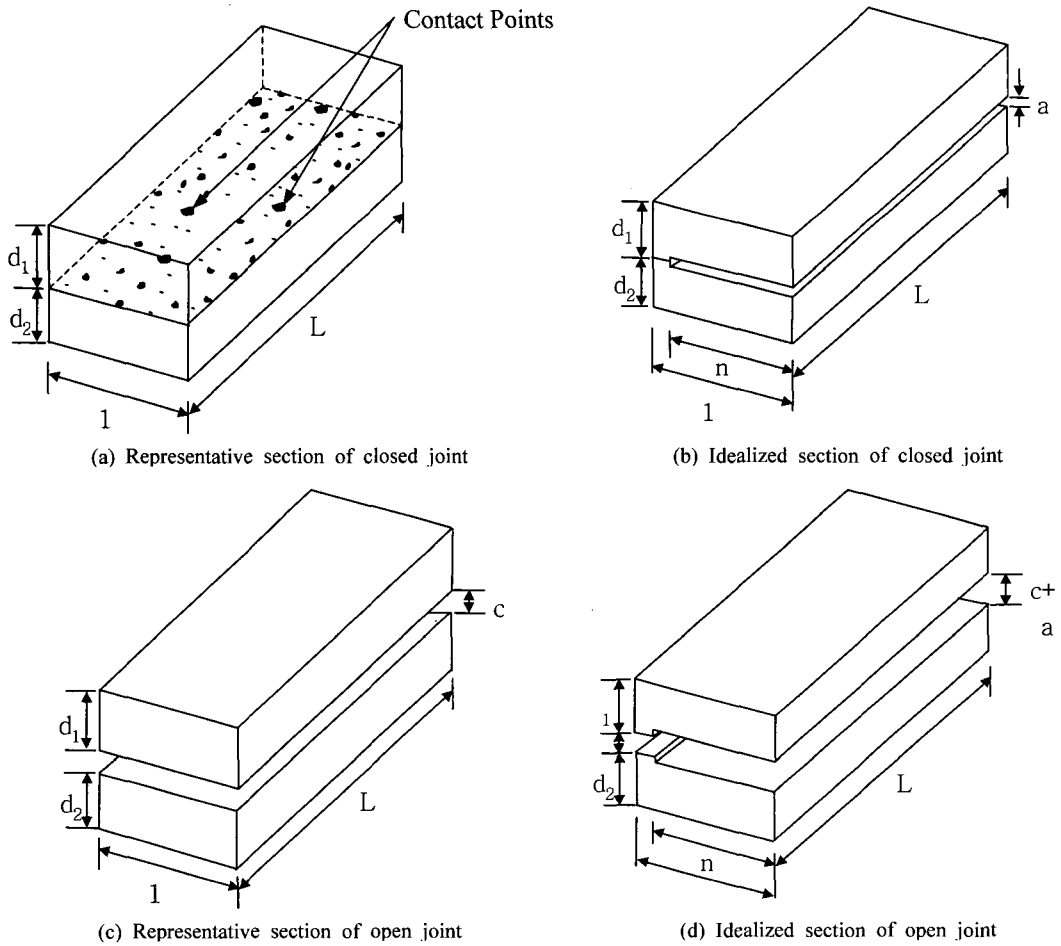

(a) Representative section of closed joint

(b) Idealized section of closed joint

(c) Representative section of open joint

(d) Idealized section of open joint

Fig. 1. Joint modeling.

a system of one-dimensional conduits of constant aperture using the approach proposed by Asgian (1988). The *apparent* aperture, b, of a conduit representing a joint depends on the contact between the joint surfaces. The joint can be classified as *closed* or *open* depending on the contact state. Consider, for instance, a closed joint with length, L, and unit width representing the interface between two contacting prismatic blocks of thickness d_1 and d_2 as shown in Fig. 1(a). Let n be the joint surface *contact porosity* (ratio between joint surface open area and total area) of the closed joint which varies between 0 and 1. The joint can be idealized as a portion of void (n) with a uniform aperture, a, and a portion of contacting solid (1-n) with vanishing aperture as shown in Fig. 1(b). The *apparent* aperture, b, of the closed joint is defined as $b = a$ for the portion of void (n).

A representative section of an open joint with length, L, and unit width is shown in Fig. 1(c). The joint represents the open interface between two prismatic blocks of thickness d_1 and d_2 separated by a gap c. The joint can be idealized as one portion of void (n) with aperture, $c + a$, and another portion of void (1-n) with aperture, c, as shown in Fig. 1(d). The *apparent* aperture, b, of the open joint consists of two components with $b_n = c+a$ for the portion of void (n) and $b_{1-n} = c$ for the other portion of void (1-n).

2.2 Water-Block Interaction Modeling of Dam

As shown in Fig. 2, the hydro-mechanical model consists of two major components: the DDA method for the rock mass and the FEM method for joint flow. The initial properties of the joints such as aperture, length, orientation, and boundary conditions from the DDA program are used to compute the piezometric heads and fluid quantities at the joints with a FEM subroutine called RFLOW. The seepage forces acting on the rock blocks are computed from the piezometric heads using a subroutine called WPRESSURE. In the DDA program, joint deformation is computed using the seepage forces. In turn, joint deformation changes the joint properties such as aperture, length, and orientation. A computational loop is followed until the results converge according to a criterion selected by the user.

In the DDA analysis, the dam was modeled as one block divided into a large number of sub-blocks. The dam foundation was modeled as several blocks formed by intersection of discontinuities, each block being itself divided into several sub-blocks. The uplift force (per unit length) at the base of the dam was determined by calculating the area under the curve representing the uplift pressure profile at the base of the dam between headwater and tailwater (Fig. 3). The DDA program with its hydro-mechanical algorithm was used to investigate the effect of different joint flow conditions on uplift: laminar or turbulent flow with hydro-mechanical coupling; laminar flow only (no turbulence is allowed) with hydro-mechanical coupling, and laminar flow uncoupled to the rock mass deformation.

Consider now a single planar joint element, i, of length L^i and constant aperture b^i as shown in Fig. 4 (a). The discharge at node k, Q^i_k and the discharge at node j, Q^i_j are equal to

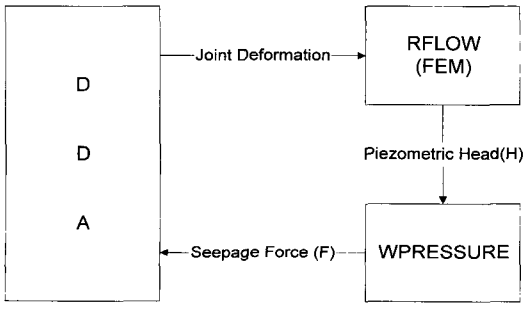

Fig. 2. Water-block interaction model.

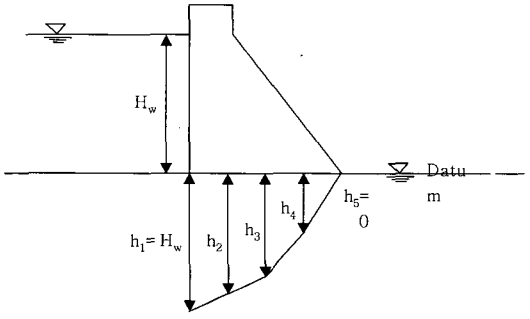

Fig. 3. Uplift force calculation method.

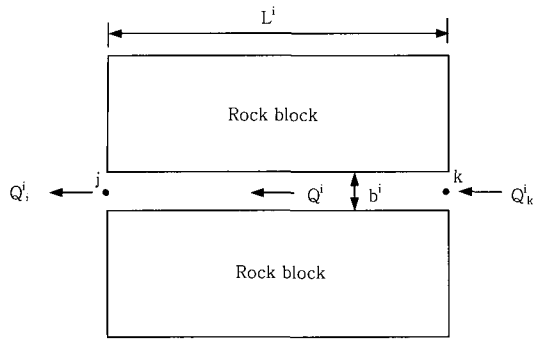

(a) Single joint element

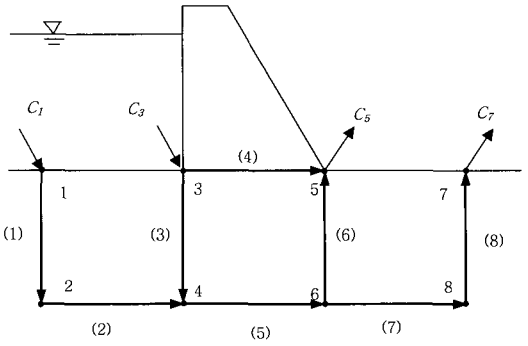

(b) Joint network

Fig. 4. Construction of total system of equations.

$$Q_k^i = T^i \Delta H^i = T^i\left(H_k^i - H_j^i\right)$$
$$Q_j^i = -T^i \Delta H^i = -T^i\left(H_k^i - H_j^i\right) \quad (1)$$

These two equations can be rewritten in matrix form as follows

$$\begin{Bmatrix} Q_k^i \\ Q_j^i \end{Bmatrix} = T^i \begin{bmatrix} 1 & -1 \\ -1 & 1 \end{bmatrix} \begin{Bmatrix} H_k^i \\ H_j^i \end{Bmatrix} \quad \text{or} \quad \mathbf{Q}^i = \mathbf{T}^i\mathbf{H}^i \quad (2)$$

where $\mathbf{Q}^i$ is the element nodal discharge vector, $\mathbf{T}^i$ the element characteristic matrix, and $\mathbf{H}^i$ the element nodal piezometric head vector.

So far, the elements in the network have been considered individually, and expressions giving the discharges in terms of the nodal piezometric heads have been developed. For a complete joint network, however, the interaction between the different elements needs to be taken into account. This implies that there must exist equilibrium at any given node of the network between the discharges of the elements connected to the node, including any inflow or outflow at that node. Consider a simplified model of a fracture network below a dam as shown in Fig. 4(b). The quantity C_j is the inflow (C_1 and C_3) or outflow (C_5 and C_7) at any node j. In general, any C_j will be positive for inflow (C_1 and C_3) and negative for outflow (C_5 and C_7). Equilibrium at any node means that the sum of the discharges of the elements connected to the node equals the inflow or outflow at that node. For any node j, the equilibrium equation can be expressed as follows:

$$\sum_i Q_j^i = C_j \quad (3)$$

where the summation runs over all elements connected to node j. By repeating the procedure for all n nodes, and using equations (2) and (3), a system of equations can be derived e.g.

$$\begin{bmatrix} T_{11} & T_{12} & \cdots & T_{1n} \\ T_{21} & T_{22} & \cdots & T_{2n} \\ \vdots & \vdots & \ddots & \vdots \\ T_{n1} & T_{n2} & \cdots & T_{nn} \end{bmatrix} \times \begin{Bmatrix} H_1 \\ H_2 \\ \vdots \\ H_n \end{Bmatrix} = \begin{Bmatrix} C_1 \\ C_2 \\ \vdots \\ C_n \end{Bmatrix} \quad \text{or} \quad \mathbf{TH} = \mathbf{C} \quad (4)$$

where $\mathbf{T}$ is the network characteristic matrix, $\mathbf{H}$ is the network piezometric head vector, and $\mathbf{C}$ is the network flow vector. Before the total system of equations (4) can be solved, it is necessary to introduce the boundary conditions for the network nodes. The boundary conditions at a given node j can be of two types; specified piezometric head (H_j) or specified flow (C_j) (Kim, 1999).

3. Numerical Model

All of the analyses presented below were conducted using a hypothetical concrete gravity dam with a height, H, of 125 m and a base length, W, of 100 m as shown in Fig. 5. The domain of analysis below the dam is 3W (300 m) wide and 1W (100 m) deep. The upstream reservoir level is 100 m and the tailwater elevation is zero. The intact rock has a unit weight of 26 kN/m^3, a Young's modulus of 3.6 GPa, and a

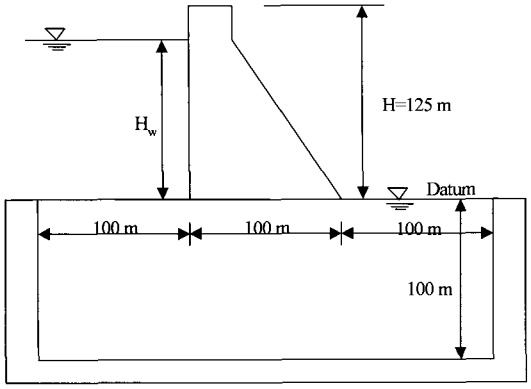

Fig. 5. Hypothetical dam and rock model.

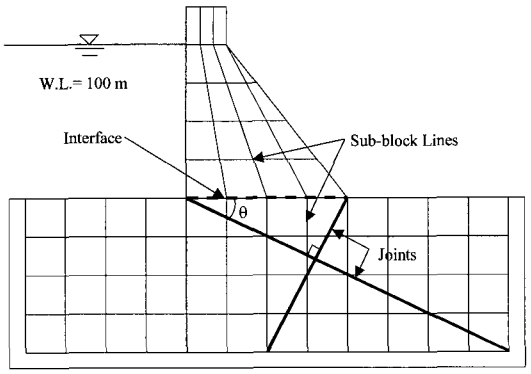

Fig. 6. Effect of joint dip angle on uplift DDA model.

Poissons ratio of 0.2. The concrete dam has a unit weight of 24 kN/m^3, a Youngs modulus of 18 GPa, and a Poissons ratio of 0.2. The water has a kinematic viscosity of 1.05 x 10^{-6} m^2/sec. The joints and the rock-concrete interface have a friction angle of 37.5° and a cohesive strength of 0.11 MPa.

4. Sensitivity to Geological Parameters

4.1 Effect of Joint Orientation

The geometry of the first example is shown in Fig. 6. Two discrete orthogonal rock joints forming a triangular wedge cut the dam foundation. The joints

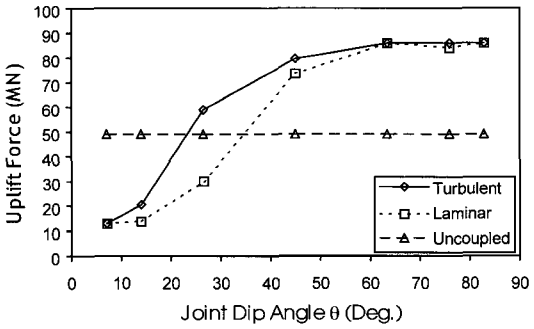

(a) Variation of uplift force with joint dip angle

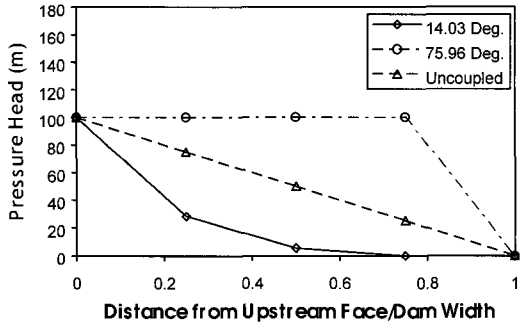

(b) Pressure head distribution along rock-concrete interface

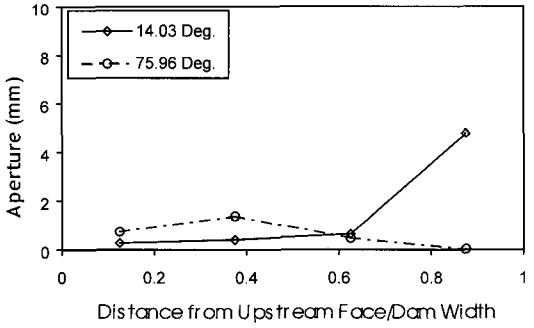

(c) Aperture variation along rock-concrete interface

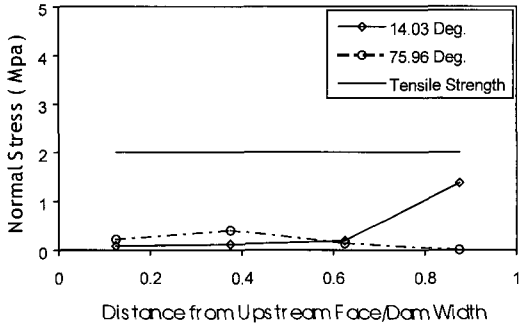

(d) Normal stress distribution along rock-concrete interface (tension positive)

Fig. 7. Effect of joint dip angle on uplift.

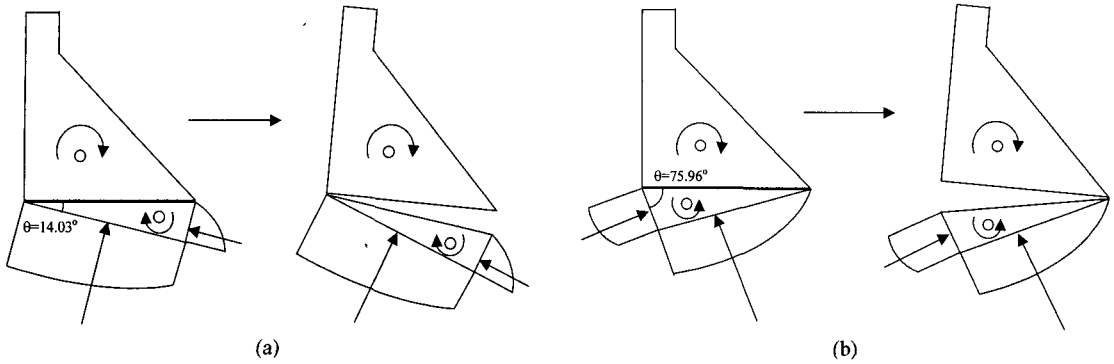

Fig. 8. Patterns of dam-rock interaction when θ = 14.03° in (a) and θ = 75.96° in (b).

and the rock-concrete interface were assumed to have an initial aperture of 0.1 mm and a tensile strength of 0.2 and 2.0 MPa, respectively. The uplift force was determined for seven values of the dip angle, θ, of the upstream dipping joint with θ = 7.12°, 14.03°, 26.56°, 45°, 63.44°, 75.96°, and 82.88°.

The variation of the uplift force with the angle, θ, is shown in Fig. 7(a) for the three joint flow conditions considered herein. This figure shows that the magnitude of the uplift force is constant for the uncoupled case but increases with the dip angle when coupling between stress and flow is taken into account. It also shows that for values of θ less than 60°, allowing for turbulence in the analysis induces larger values of the uplift force.

Fig. 7(b) and 7(c) show respectively the pressure head distribution and final aperture distribution along the rock-concrete interface for two values of the dip angle (i.e. θ = 14.03° and 75.96°) assuming hydro-mechanical coupling. Also shown for comparison in Fig. 7(b) is the pressure head distribution for the uncoupled case corresponding to the classical linear variation from full reservoir head to tailwater.

The results in Figs. 7(b) and 6(c) indicate that the two values of the dip angle create two different patterns of rock-dam interaction as shown in Figs. 8(a) and 8(b). In both cases, the dam tends to rotate clockwise. When the upstream joint dips at a small angle θ = 14.03°, the triangular wedge under the dam tends to rotate clockwise due to the water pressure along the joints (Fig. 8(a)). As the dam and the wedge rotate, Fig. 7(c) indicates that the aperture of the interface increases from the heel to the toe of the dam. This opening of the interface in the flow direction induces a large dissipation of pressure head on the dam upstream side and results in a head distribution less than the classical linear distribution as shown in Fig. 7(b). The opposite pattern can be observed when the upstream joint dips at a large angle θ = 75.96°. In that case, the wedge below the dam tends to rotate counter-clockwise (Fig. 8(b)). As the dam and the wedge rotate, Fig. 7(c) indicates that the aperture of the interface decreases from the heel to the toe of the dam. This closing of the interface in the flow direction induces a build-up of pressure head on the dam upstream side and results in a head distribution larger than the classical linear distribution as shown in Fig. 7(b).

Fig. 7(d) shows the normal stress distribution along the rock-concrete interface for the two values of the dip angle (i.e. θ = 14.03° and 75.96°) assuming hydro-mechanical coupling. The results in Fig. 7(d) indicate that, in both cases, the tensile stresses along the entire interface are smaller than the tensile strength of the interface. Thus, slight opening and no separation occur along the rock-concrete interface.

Fig. 7(a) also shows that for values of the dip angle less than 60°, inclusion of turbulence yields larger values of the uplift force when coupling between flow and stress is taken into account. This can be explained by considering the head distribution along the joints forming the wedge below the dam and the final

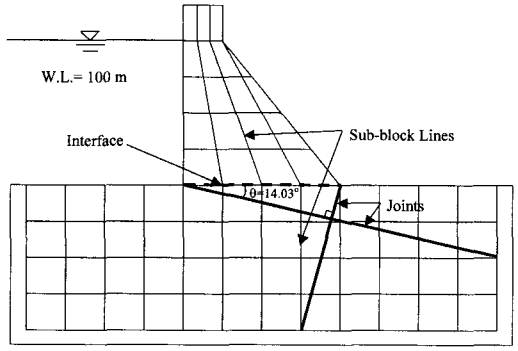

(a) DDA model

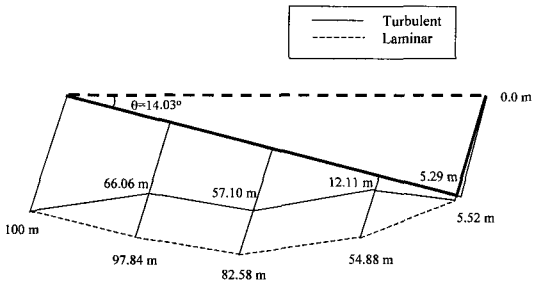

(b) Pressure head distribution along the rock wedge at the base of the dam

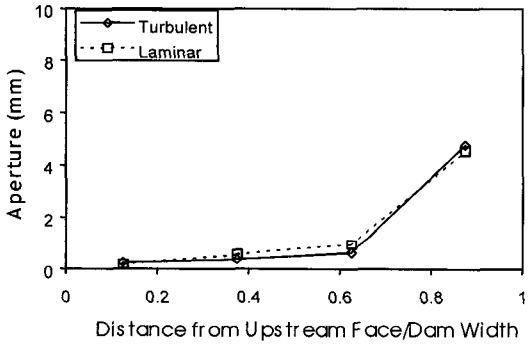

(c) Aperture variation along rock-concrete interface

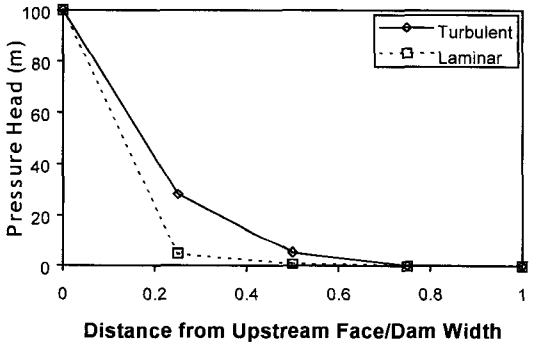

(d) Pressure head distribution along rock-concrete interface

Fig. 9. Comparison between turbulent and laminar flow when θ = 14.03°.

aperture distribution along the rock-concrete interface. As an example, consider the case when θ = 14.03° and the geometry of Fig. 9(a). Fig. 9(b) and 9(c) and 9(d) show respectively the head distribution along the wedge, and the final aperture distribution and pressure head distribution along the rock-concrete interface for laminar flow only and when turbulence is allowed to occur. In both cases, it appears that the aperture of the interface increases in the flow direction with slightly less interface opening when turbulence exists (Fig. 9(c)), thus resulting in higher values of the head along the rock-concrete interface (Fig. 9(d)) and larger uplift.

4.2 Effect of Joint Spacing

The effect of joint spacing on uplift was investigated for the geometry of Fig. 10. The rock mass is cut by two orthogonal joint sets with equal spacing, S. Five values of the joint spacing were considered corresponding

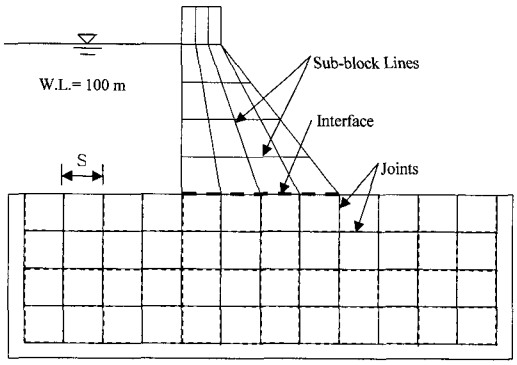

Fig. 10. Effect of joint spacing on uplift DDA model.

to a spacing-dam base length ratio S/W = 0.125, 0.25, 0.5, 1.0 and 2.0. The joints and the rock-concrete interface were assumed to have an initial aperture of 0.1 mm and a tensile strength of 2.0 MPa.

Fig. 11(a) shows the variation of the uplift force with the joint spacing for coupled flow (allowing for

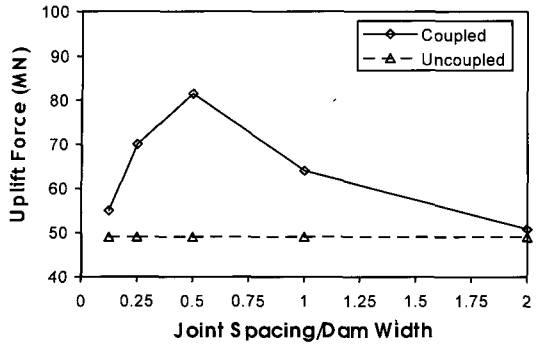

(a) Variation of uplift force with joint spacing

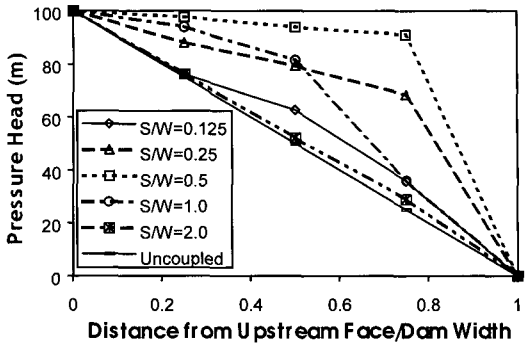

(b) Pressure head distribution along rock-concrete interface

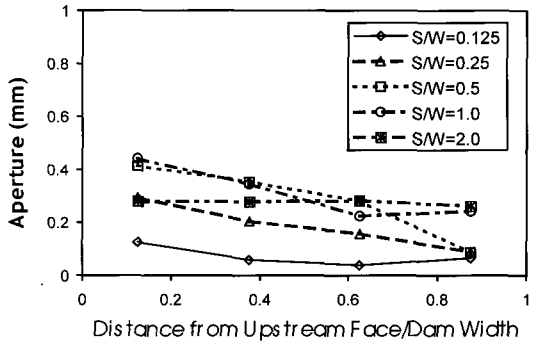

(c) Aperture variation along rock-concrete interface

Fig. 11. Effect of joint spacing on uplift.

turbulence) and uncoupled flow. In the uncoupled case, uplift is independent of the joint spacing. On the other hand, when coupling between stress and joint flow is considered, the uplift force is much larger and reaches a maximum value when S/W = 0.5.

The trend in Fig. 11(a) can be explained by considering the final aperture distributions along the rock-concrete interface shown in Fig. 11(c). All distributions indicate that the aperture of the rock-concrete interface decreases from the heel to the toe of the dam. The closing of the interface in the flow direction induces a build-up of pressure head on the dam upstream side and results in a head distribution larger than the classical linear distribution as shown in Fig. 11(b). However, the amount of closing of the interface and the corresponding pressure head distribution depend on the value of S/W, i.e. on the relative size of the foundation rock blocks with respect to the dam base length. The largest variation in aperture along the rock-concrete interface and the maximum pressure head take place for S/W = 0.5. On the other hand, for S/W = 0.125 (very fractured rock mass) and 2.0 (very competent rock mass), the interface aperture does not show much variation and the pressure head distribution is slightly higher than the classical linear distribution. It is noteworthy that these two extreme cases result in almost the same amount of uplift but the quantity of seepage along the interface differs. The flow rate along the interface is equal to 4.35×10^{-7} m^3/s when S/W = 0.125 and is 39 times larger and equal to 1.68×10^{-5} m^3/s when S/W = 2. This example also shows that a dam foundation consisting of small blocks is quite flexible as the blocks can move more freely when the dam interacts with the foundation rock. As a result, the aperture of the interface between the rock and the dam tends to be more uniform.

4.3 Effect of Major Joint Location

The geometry of the problem is shown in Fig. 11

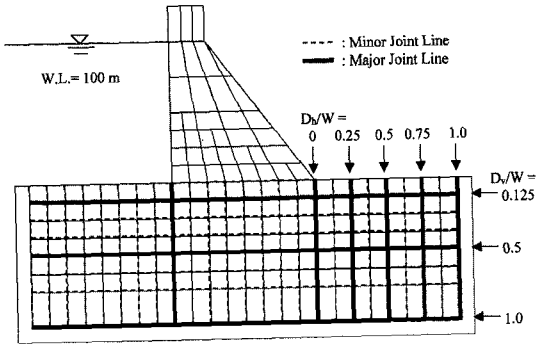

Fig. 12. Effect of major joint on uplift-DDA model.

where the rock mass is now cut by two systems of orthogonal joints classified as minor and major. The minor joints are equally spaced with a spacing of 12.5 m. The rock mass is also cut by a major horizontal joint located at a depth, D_v, and two major vertical joints, one always fixed at the heel of the dam and the other located at a distance, D_h, from the toe of the dam.

The uplift force was determined for three different depths of the major horizontal joint (D_v/W = 0.125, 0.5, 1.0) and five locations of the downstream vertical joint (D_h/W = 0, 0.25, 0.5, 0.75, 1.0). In all the analyses, the minor joints and the rock-concrete interface were assumed to have an initial aperture of 0.1 mm and a tensile strength of 2.0 MPa. The major joints were assumed to have an initial aperture of 1.0 mm and a tensile strength of 0.7 MPa.

Fig. 13(a), 13(b) and 13(c) show the variation of the uplift force with D_h/W when D_v/W is equal to 0.125, 0.5 and 1.0, respectively. Three joint flow conditions are considered. When the major horizontal joint is at shallow depth (D_v/W = 0.125), Fig. 13(a) indicates that uplift increases with the distance between the toe of the dam and the downstream major vertical joints, regardless of the assumed joint flow condition. However, the uplift force assuming laminar flow only is always higher than that when turbulence is taken into account since more energy losses are associated with turbulent flow.

Since, in this example, the major joints have an aperture ten times that of the minor joints, the major joints control most of the flow in the dam foundation. As D_h/W increases (i.e. as the horizontal flow path length increases between headwater and tailwater), more head loss occurs and the likelihood of having turbulent flow decreases. As a result, the uplift force assuming turbulent flow approaches its value assuming laminar flow only as shown in Fig. 13(a). This figure also indicates that uplift is always larger when coupling between stress and flow is considered.

As the major horizontal joint is located deeper below the dam, the length of the flow path along the major joints below the dam increases which makes turbulence less likely to occur. When D_v/W = 0.5 and 1.0, Fig. 13(b) and 13(c) show that turbulence has no effect on the uplift force. These two figures also indicate that as the major horizontal joint is located deeper below the dam, the hydro-mechanical coupling becomes less critical and the magnitude of the uplift force at the base of the dam decreases. It is likely that at depths greater than the dam base length (D_v/W > 1), flow along major horizontal joints should have a

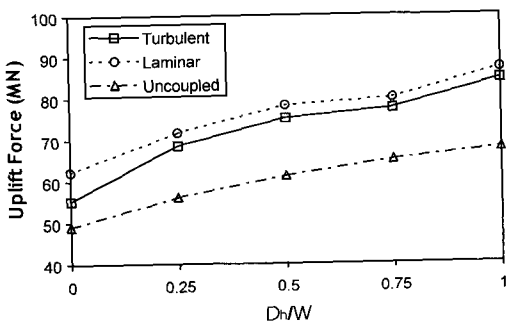

(a) D_v/W = 0.125

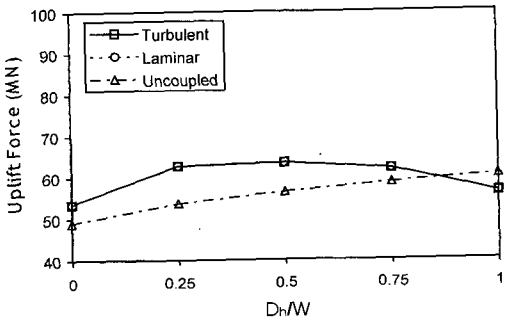

(b) D_v/W = 0.25

Fig. 13. Effect of major joint location on uplift.

negligible effect on the magnitude of the uplift force.

5. Conclusions

This paper presents an alternative method of predicting uplift and seepage at the base of concrete gravity dams using the DDA method with a new hydro-mechanical algorithm.

A sensitivity analysis was carried out to study the importance of several uncontrollable and controllable parameters on uplift. The uncontrollable parameters are geological and include the orientation, spacing, and location of discontinuities. The controllable parameters include the location and diameter of foundation drains.

The results of the sensitivity analysis show clearly that uplift at the base of concrete gravity dams founded on jointed rock is quite different from that assuming that the rock mass behaves as an equivalent continuum. The linear or bi-linear pressure distribution used in the current practice of dam design is more an exception than a rule when discontinuities control flow in dam foundations. In fact, uplift at the base of concrete gravity dams can be much larger than that predicted with the classical linear or bi-linear pressure assumption.

The results of the analysis also indicate that hydro-mechanical coupling needs to be considered as it reflects better the deformation of a rock mass associated with the interaction between a dam and its foundation. Compared to a continuum, jointed rock masses experience larger displacements through block translation and rotation. Such displacements induce drastic changes in the rock mass hydraulic properties that are critical when estimating uplift.

Finally, this paper shows that, in general, the DDA program with the hydro-mechanical algorithm can be used as a practical tool in the design of gravity dams built on fractured rock masses.

References

1. Asgian, M. I. 1988. A numerical study of fluid flow in deformable, naturally fractured reservoirs., Ph.D. thesis, University of Minnesota.
2. Casagrande, A. 1961. Control of Seepage through Foundation and Abutments of Dams. Geotechnique. XI: 161-181.
3. Grenoble, B. A. 1989. Influence of Geology on Seepage and Uplift in Concrete Gravity Dam Foundations. Ph.D. thesis. University of Colorado at Boulder.
4. Illangasekare, T.H., Amadei, B. & Chinnaswamy, C. 1991. Uplift Reduction using Drains. Water Power 91, 1388-1397.
5. Jang, H. I. 2001. Development of a Three-dimensional Discontinuous Deformation Analysis Technique and its Application to a Failed Rock Slope. Ph.D. Dissertation. Seoul National University.
6. Kim, Y. I. 1999. Modeling the Water-Block Interaction with Discontinuous Deformation Analysis Method. Journal of Korean Society for Rock Mechanics, Tunnel & Underground Vol. 9, 149-157.
7. Kim, Y. I., Amadei, B. & Pan, E. 1998. Modeling the Effect of Water, Excavation Sequence and Reinforcement on Tunnel Stability. Proc. 3rd NARMS. Cancun, Mexico, 681-682.
8. Lin, C.T. 1995. Extensions to the Discontinuous Deformation Analysis for Jointed Rock Masses and Other Block Systems. Ph.D. thesis. University of Colorado at Boulder.
9. Louis, C. 1969. A study of groundwater flow in jointed rock and its influence on the stability of rock masses. Imperial College, Rock Mechanics Research Report, No. 10.
10. Rouainia, M., Pearce, C., Bicanic, N., Lewis, H., Couples, G. 2001. Hydro-mechanical Modelling of Fracture Porous Media with Discontinuous Deformation Analysis. Association for Computational Mechanics in Engineering. 69-74.
11. Serafim, J. L. & del Campo, A. 1965. Interstitial Pressures on Rock Foundations of Dams. ASCE J. Soil Mech. Found. Div., 91(4): 959-969..
12. Shi, G.H. 1988. Discontinuous Deformation Analysis: A New Numerical Model for the Statics and Dynamics of Block Systems. Ph.D. thesis. University of California, Berkeley.
13. Stuart, W. H. 1963. Influence of Geological Conditions on Uplift. Trans. Am. Society of Civil Engineers. 128: 765-780.
14. Terzaghi, C. 1929. Effect of Minor Geologic Details on the Safety of Dams. AIME Technical Publication. 215: 31-44.

김 용 일

1986년 서울대학교 공과대학 토목공학과 공학사
1988년 서울대학교 대학원 토목공학과 공학석사
1998년 미국 University of Colorado-Boulder 토목공학과 공학박사
Tel: 02-2288-5241
E-mail: 8915364@mail.dwconst.co.kr
현재 (주)대우건설 토목기술 1팀 차장